Supplementary Information

Supplementary Note 1. Terahertz electric-field dependence of reflectivity changes

To clarify whether the observed reflectivity changes by terahertz electric fields originate from the third-order optical nonlinearity, we measured $\Delta R(t_{\mathrm{d}} = 0\ \mathrm{ps})/R$ for various amplitudes of the terahertz electric fields $E_{\mathrm{THz}}(0)$. In Supplementary Figure 1, we show the $E_{\mathrm{THz}}(0)$ dependence of $|\Delta R(t_{\mathrm{d}} = 0\ \mathrm{ps})/R|$ at probe energies of 0.72 eV and 0.80 eV. Both data items are proportional to the square of $E_{\mathrm{THz}}(0)$ up to ~110 kV cm^{-1}. This demonstrates that the observed $\Delta R/R$ signals can be attributed to the third-order optical nonlinearity.

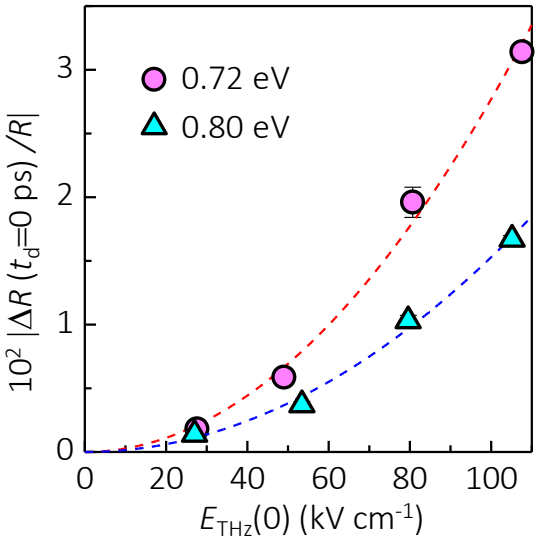

Supplementary Figure 1. Terahertz-electric-field $E_{\mathrm{THz}}(0)$ dependence of the reflectivity changes $|\Delta R(t_{\mathrm{d}} = 0\ \mathrm{ps})/R|$ at 0.72 eV and 0.80 eV (open circles and triangles, respectively). Broken lines show the quadratic dependences on $E_{\mathrm{THz}}(0)$. The error bars indicate the standard deviation.

Supplementary Note 2. Kramers–Kronig transformation of reflectivity-change spectra

To perform the Kramers–Kronig (KK) transformations of the $\Delta R/R$ spectra, we extrapolated the $\Delta R/R$ spectra since the measurement range was limited. In the $\Delta R/R$ spectra obtained by terahertz-pulse-pump optical-reflectivity-probe spectroscopy, the measurement range was 0.48 eV to 1.08 eV. Below (above) the lower (higher) energy bound of the measured range, we linearly extrapolated the data using the lowest (highest) two measurement points and set $\Delta R/R$ to be zero after $\Delta R/R$ reached zero. We also made the liner interpolation in the $\Delta R/R$ spectra experimentally obtained from 0.48 eV to 1.08 eV since the number of measurement points was insufficient to perform the KK transformation.

In the $\Delta R/R$ spectra obtained by optical-pump optical-reflectivity-probe spectroscopy, the measurement range was 0.082 eV to 2.17 eV. Below the lower energy bound of the measurement range, we used an $\Delta R/R$ value of 0.082 eV. Above the higher energy bound, we linearly extrapolated the data using the highest two measurement points and set $\Delta R/R$ to be zero after $\Delta R/R$ reached zero. We also linearly interpolated the $\Delta R/R$ spectra from 0.082 eV to 2.17 eV.

Supplementary Note 3. Excitation photon density dependence of exciton-biexciton transition

To clarify how the dynamics of biexcitons depends on the density of excitons generated by the pump pulse, we measured the excitation photon density x_{ph} dependence of reflectivity changes $\Delta R/R$ at 0.58 eV, which corresponds to the peak

energy of the exciton-biexciton transition. Supplementary Figure 2 shows $\Delta R/R$ at 0.58 eV (t_{d}= 1 ps) as a function of x_{ph}. The magnitudes of $\Delta R/R$ is proportional to x_{ph} below $x_{\mathrm{ph}} = 0.015$ photons per ET molecule (ph/ET) and then saturated. The observed saturation of the signals for $x_{\mathrm{ph}} > 0.015$ ph/ET suggests that under the presence of a high density of excitons or equivalently doublon-holon pairs, the subsequent probe pulse is difficult to form a stable biexciton. We consider that a high density of excitons would destabilize a biexciton by modifying the long-range Coulomb interactions possibly through screening or many-body effects. Taking these facts into account, we investigated the exciton-biexciton transition in the low-fluence excitation condition with $x_{\mathrm{ph}} = 0.0015$ ph/ET.

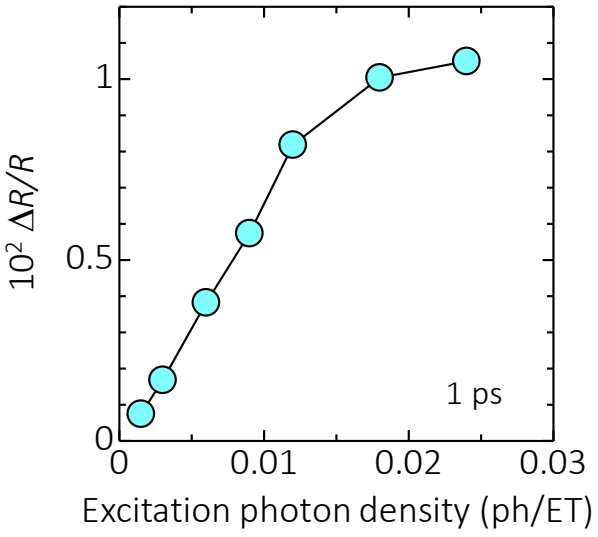

Supplementary Figure 2. Reflectivity changes $\Delta R/R$ at 0.58 eV (the delay time t_{d} =1 ps) as a function of the excitation photon density x_{ph}. The error bars are smaller than the data points.

Supplementary Note 4. Excitation-photon-energy dependence of time evolutions of reflectivity change

To distinguish between the coherent response and the bleaching signal owing to the real excitation of excitons, we compared the time evolution of $\Delta R/R$ by the resonant excitation to the lowest odd-parity exciton and that by the higher-energy excitation with 1.55 eV as previously reported[1]. These are indicated by the green and red solid lines, respectively, in Supplementary Figure 3. In the case of the 1.55-eV excitation, no ultrafast component can be observed around the time origin in contrast to the case of the resonant exciton excitation. This indicates that the ultrafast component of $\Delta R/R$ does not originate from the real excitation of excitons nor carriers but the coherent response. On the other hand, both time evolutions include a slower decay component with a relaxation time of several ps, so this can be ascribed to the real excitation of excitons or carriers.

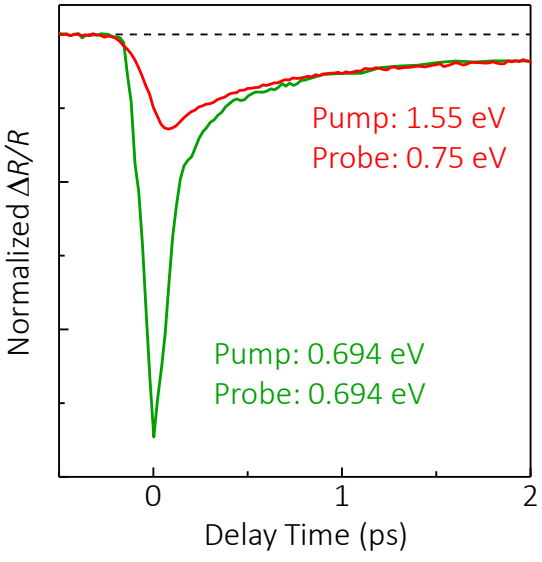

Supplementary Figure 3. Time evolutions of the reflectivity change at 0.694 eV with the resonant excitation to the lowest odd-parity exciton (green solid line) and at 0.75 eV with the higher energy excitation with 1.55 eV (red solid line)[1].

Supplementary Note 5. Analyses of coherent oscillations on photoinduced reflectivity changes

To analyse the coherent oscillations on the time evolutions of $\Delta R/R$ obtained by the optical-pump optical-reflectivity-probe measurements, we derived the oscillatory components by applying a high-pass Fourier filter with a cut-off frequency of 1.6 THz to the $\Delta R/R$ data. To exclude the contribution of the coherent response around the time origin, we used the data only for $t_{\mathrm{d}} > 0.2$ ps. We next performed fitting analyses of the oscillatory components thus obtained using eq. (7) as described in the main text. In these analyses, we used the common values of decay time $\tau = 2.0$ ps and oscillation frequency $\omega_{\mathrm{OSC}} = 82\ \mathrm{cm}^{-1}$.

Supplementary Note 6. Evaluation of decay dynamics of excitons

To evaluate the decay dynamics of the exciton, we performed the fitting analysis of the time evolutions of $\Delta R/R$ at 0.694 eV and 0.96 eV by using the following function convolved with the Gaussian profile corresponding to the time resolution (150 fs).

$$\Delta R/R\,(t_{\mathrm{d}}) = A\delta(t) + A_{\mathrm{fast}}\exp\left(-\frac{t_{\mathrm{d}}}{\tau_{\mathrm{fast}}}\right) + A_{\mathrm{slow}}\exp\left(-\frac{t_{\mathrm{d}}}{\tau_{\mathrm{slow}}}\right) \qquad \text{(S1)}$$

The first term represents the coherent response and its magnitude is denoted by A. $\delta(t_{\mathrm{d}})$ is the delta function. The second (third) term shows the fast (slow) decay component of excitons, the magnitude and decay time of which are denoted by A_{fast} (A_{slow}) and τ_{fast} (τ_{slow}), respectively.

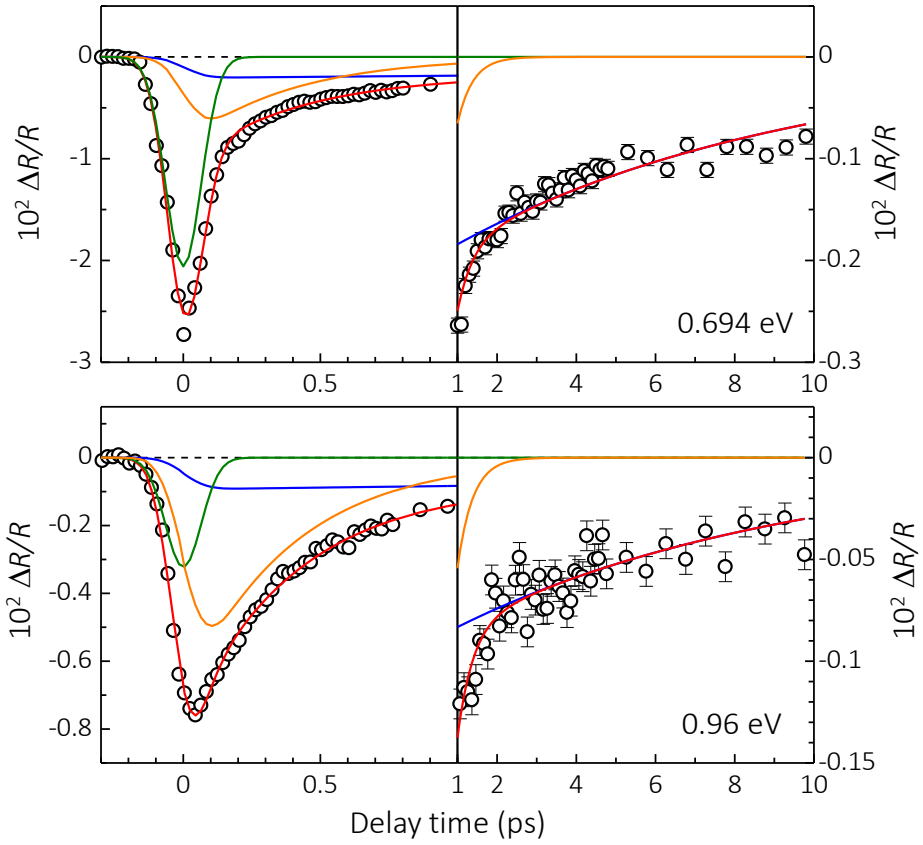

Supplementary Figure 4. Time evolutions (circles) and fitting curves (red lines) of reflectivity changes at 0.694 and 0.96 eV. The green, orange, and blue lines represent the coherent response, the fast decay component, and the slow decay component, respectively. The error bars indicate the standard deviation.

The time evolutions of $\Delta R/R$ at 0.694 eV and 0.96 eV, and the fitting curves are shown in Supplementary Fig. 4. Both time evolutions are well reproduced by the fitting curves as shown by the red solid lines with the common values of τ_{fast}=0.39 ps and τ_{slow}=8.6 ps. The time evolution of the coherent response, the fast decay component, and the slow decay component are also shown by the green, orange, and blue lines, respectively, in the same figure.

The positive $\Delta R/R$ signal at 0.58 eV due to the exciton-biexciton transition also gives the information about the decay dynamics of exciton. As mentioned in the main text, the $\Delta R/R$ signal at 0.58 eV will include the contribution of the negative $\Delta R/R$ component due to the coherent response around the time origin, so that we analysed only the data for $t_{\mathrm{d}} > 1$ ps using the following formula including only the third term in Eq. (S1).

$$\Delta R/R\,(t_{\mathrm{d}}) = A_{\mathrm{slow}}\exp\left(-\frac{t_{\mathrm{d}}}{\tau_{\mathrm{slow}}}\right) \tag{S2}$$

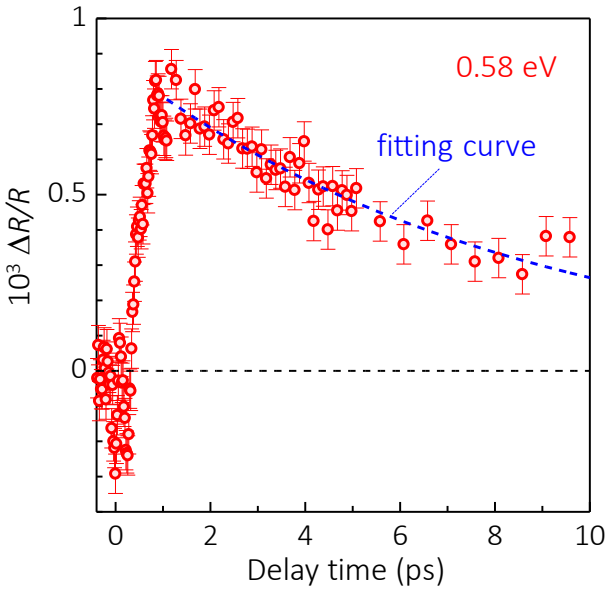

Supplementary Figure 5. A time evolution of the reflectivity change at 0.58 eV (red open circles) and a fitting curve (blue broken line). The error bars indicate the standard deviation.

In Supplementary Fig. 5, we show the time evolution of $\Delta R/R$ at 0.58 eV and the fitting curve. The data is well reproduced by Eq. (S2) as shown by the blue broken line. The decay time τ_{slow} is 8.3 ps, which is almost the same as the values (8.6 ps) obtained

by the fitting analyses of the data at 0.694 eV and 0.96 eV. It is reasonable since the time evolution of the exciton-biexciton transition reflects the decay characteristic of excitons.

Supplementary References

1. Uemura, H., Matsuzaki, H., Takahashi, Y., Hasegawa, T., & Okamoto, H. Ultrafast charge dynamics in one-dimensional organic Mott insulators. *J. Phys. Soc. Jpn.* **77**, 113714 (2008).